Controlling surface plasmon polaritons by a static and/or time-dependent external magnetic field

V. Kuzmiak, S. Eyderman, and M. Vanwolleghem

Phys. Rev. B **86**, 045403 — Published 5 July 2012

DOI: 10.1103/PhysRevB.86.045403

Controlling surface plasmon-polaritons by static and/or time-dependent external magnetic field.

V. Kuzmiak[1] , S. Eyderman[1], and M. Vanwolleghem[2]

[1]Institute of Photonics and Electronics, v.v.i. Czech Acad. of Sciences,
Chaberska 57, 182 51 Praha 8, Czech Republic.
[2] Institut d'Elecronique Fondamentale, CNRS UMR8622, Université Paris 11, 91405 Orsay, France

Abstract : We have demonstrated numerically by using of Fourier Modal Method(FMM) that the interface between a metal and a uniformly magnetized two-dimensional photonic crystal fabricated from a transparent dielectric magneto-optical(MO) material possesses a one-way frequency range in which a surface plasmon-polariton(SPP) is allowed to propagate only in one direction. The time-reversal symmetry breaking is implied by the MO properties of the photonic crystal material, namely bismuth iron garnet(BIG), which may be magnetically saturated by fields of the order of tens of mT. The results obtained by FMM have been validated by a theoretical model and a standard plane-wave method that yield separately a nonreciprocal dispersion relation for the SPP and the band structure of the 2D MOPhC, respectively. These spectra represent the key characteristics assuring the functionality of the one-way waveguide associated with the both underlying mechanisms, namely time-reversal symmetry breaking and a suppression of disorder-induced backscattering. By using a generalized finite-difference time-domain(FDTD) method, which allows studying the propagation of electromagnetic(EM) waves through media with a tensor MO permittivity, we studied transport properties of the one-way waveguide. We examined the influence of specific types of boundary conditions on one-way functionality in the presence of a static external magnetic field and have shown that the SPP can be dynamically controlled by applying a time-dependent magnetic field. By evaluating the Fourier transform of the energy density we have analyzed the behavior of the field patterns observed in the waveguide in the case of ac magnetic field, and have interpreted new and

interesting features associated with the redistribution of the EM field that may offer new mechanisms for dynamical control of SPP flow.

PACS. 42.70.QS, 41.20.Jb.

1. INTRODUCTION.

Photonic crystals as photonic analogues of semiconductors[1]-[2] offer an unprecedented ability to manipulate light, which has led to many applications in nanophotonics. The equivalence between the behavior photons in photonic crystals and that of electrons in electronic systems have been systems has been recently extended by Raghu and Haldane [3] who predicted photonic analogues of quantum chiral edge states [4]. These EM modes that are confined at the edge of certain 2D MO photonic crystals, which break time-reversal symmetry, can propagate in only one direction, determined by the direction of an applied dc magnetic field. Since the time-reversed modes do not belong to the spectrum of the system the backscattering is completely suppressed due to the absence of backpropagating modes. However, this concept relies on a TE gap opening around a Dirac point in a triangular lattice via time-reversal asymmetry by the use of gyroelectric materials. It has been argued by Wang [5] that these gyroelectric corrections are rather weak, and as a result, the gap is not robust against disorder, and the resulting chiral edge modes scatter easily into bulk modes. To realize one-way chiral edge states experimentally he proposed to use gyromagnetic materials having orders of magnitude stronger effects. Using a photonic crystal consisting of a 2D periodic arrangement of ferrite rods, Wang *et al*. [6] observed such photonic edge states in a 2D MO photonic crystal at gigahertz frequencies. Ochiai proposed theoretically a similar effect in a photonic graphene analogue [7]. Obviously both examples profit greatly from the much stronger gyromagnetic effects (on the permeability tensor) that are

only accessible at microwave frequencies. At infrared and optical frequencies, there are only much weaker gyro-electric effects available.

The experimental demonstration of the correspondence between photonic edge states and chiral edge states found in integer Hall effect opened the door to practical applications of non-reciprocal photonic crystals. Unlike traditional designs for nonreciprocal devices in which MO materials have been used as the basis for optical isolators and circulators in the bulk optics regime, non-reciprocal photonic crystals can provide means to extend MO-based nonreciprocal effects to domain of integrated photonics and allow to develop a compact integrated analogs of one-way electronic devices such as diodes and transistors. On the other hand, the possibility of attaining ultra-low-loss light propagation with both absorption and scattering losses suppressed may be employed in construction of the ideal optical waveguide made of low-loss hollow core for telecom applications [8]. The prediction of Haldane of Raghu[3] as well as its experimental verification by Wang *et al*.[6] are based on a strict condition that requires breaking both space- and time-reversal symmetry [9] in order to ensure spectral nonreciprocity $\omega(-k) \neq \omega(k)$. To satisfy limitations on symmetry several different approaches based on proper spatial arrangement of magnetic and dielectric components with strong anisotropy have been proposed to achieve non-reciprocity in 1D MOPhCs[10]-[12]. More realistic 1D configuration in which nonreciprocity is achieved without anisotropy and with uniform magnetization has been proposed recently [13]. Simultaneously, nonreciprocity attracted great deal of interest in two dimensional structures. Various nonreciprocal devices such as one-way waveguides [14-15] and circulators [16-17] were proposed. Namely, the existence of one-way frequency range in a waveguide formed at the interface between a semi-infinite photonic crystal and a semi-infinite metal region under a static magnetic field has been demonstrated theoretically [14]. A possibility to achieve compact optical on-chip waveguide isolation has been demonstrated by Takeda [15] by using nonreciprocal waveguides fabricated from a magneto-optic material in which spatial inversion symmetry is broken. Similarly by judiciously reducing the symmetry of

the motif of the uniformly magnetized 2D MOPhC a unidirectional PhC mirror has been proposed, that perfectly reflects the light only in one direction of propagation for a total one-way mirror thickness of just tens of wavelengths [18]. Besides the 2D structures including in which nonreciprocity is a local property of guided or defect modes [14-17], the concept of 1D nonreciprocal geometry proposed in Ref. 13 has been extended to a 2D geometry to aim to design structures with nonreciprocity as a bulk property [19].

In several papers published recently[20-24] authors claimed nonreciprocity on the basis of various effects observed in the behavior electromagnetic propagation in linear, time-independent structures consisting of materials described by symmetric (i.e. reciprocal) permittivities and/or permeabilities. It is well known that the Lorentz reciprocity theorem does not allow nonreciprocal behavior in such structures. Therefore, assigning the observed effects to Lorentz nonreciprocity obviously arise from a faulty interpretation of numerical or experimental data. Specifically, it has been argued by one of us (M.V.) [25] that in the interpretation of the behavior observed in silicon photonic circuit based on asymmetric mode conversion observed experimentally [24] the term "nonreciprocal" has been used incorrectly. Based on the validity of the Lorentz nonreciporocity theorem statement we believe that the interpretation of the effects observed in Refs. [20-24] merit a critical reading.

In this paper we propose a modified one-way waveguide that takes advantage of the one-way waveguide configuration considered in Ref. 14 and have shown that the SPP can be dynamically controlled by applying a time-dependent magnetic field. In our configuration we introduced an additional flexibility that enables overcoming a major drawback of previously the reported design, namely the need for an unrealistically high external magnetic field (~ several T) in order to achieve a sizable one-way bandwidth. The system we consider consists of a transparent dielectric MO material and a metal region. The nonreciprocity at the interface is introduced by the MO properties of the photonic crystal material assumed to be bismuth iron garnet a ferrimagnetic oxide that can be magnetically saturated by fields of the order of tens of mT and

that has been reported to have record MO properties from the visible throughout the near IR [26]. Our paper is organized as follows: In Section II we implement a simple analytical model [27] that is used to calculate the nonreciprocal dispersion relation of the surface plasmon-polariton propagating along the interface between the metal and a homogeneous medium fabricated from the MO material. This dispersion relation which possesses one-way frequency range is superimposed on the band structure of the 2D MOPhC that has been calculated by a standard plane-wave method. In Section III we describe a generalized FDTD algorithm that allows calculating the propagation of EM waves through media with a tensor magneto-optic permittivity. In Section IV we present the results of numerical simulations that demonstrate the possibility of controlling the propagation of the SPP along the MOPhC/metal interface in the presence of a static and/or a time-dependent external magnetic field. We conclude in Sec. V with a discussion of the feasibility of employing such a design to fulfill non-reciprocal optical functionalities of an optical isolator and an optical circulator in a competitive integrated version, and of possible directions for further investigations of one-way waveguide systems.

2. **ONE-WAY WAVEGUIDE MODEL.**

In this paper we consider a waveguide that is formed by the interface between a metal characterized by the Drude free-electron model and a 2D magneto-optic photonic crystal subject to an externally applied magnetic field that is perpendicular to the plane of propagation – see Fig. 1. We show that such a configuration constitutes a non-reciprocal system provided that the frequency of the surface plasmon frequency propagating at the interface between the metal and the MOPhC lies within the band gap of the photonic crystal. The design of the structure relies on both the presence of the surface plasmon-polariton, which is independent of time-reversal symmetry breaking and the 2D magneto-optic photonic crystal under a static magnetic field. The role of the MOPhC is two-fold: it provides the non-reciprocity that is induced by the magneto-optic material

from which the photonic crystal is fabricated, while its periodicity gives rise to the band gap from which the radiation modes are eliminated, such a waveguide suppresses disorder-induced backscattering. To this end it is important to point out that the absence of backpropagating mode is of crucial importance in nanodevices where the effects of disorder are dramatically sensitive to time-reversal symmetry properties. While in reciprocal devices in the presence of disorder, the forward and backward propagating modes that exist at given frequency, scatter into each other and give rise to backreflection, which can reduce forward transmission. Such backreflection can be of crucial importance in slow light systems where the scattering losses dominate over all other lossy mechanism in the limit of vanishing group velocity v_g.

2. A **BAND STRUCTURE CALCULATION.**

The presence of the band gap is a key feature of the studied one-way waveguide since it prevents backscattering via the reciprocal radiation continuum. Therefore, information on the spectrum of the Bloch modes is essential for the theoretical description of the system. As has been pointed out in Ref. 14, in order to achieve a true one-way propagation it is crucial that within a certain frequency range there appears a photonic band that has a single sign for its group velocity over the whole first Brillouin zone. This implies a band structure asymmetry, $\omega(-k) \neq \omega(k)$ and the simultaneous satisfaction of the Bloch theorem $\omega(-\pi/a) = \omega(\pi/a)$, since the two equal frequency modes belong to different bands. To describe the underlying dispersion relation of the one-way EM waveguide we previously implemented a MO aperiodic Fourier Modal Method that has been described in Ref. 28. We have shown that by using an eigenmode scattering matrix technique one can deduce the response of an arbitrary finite system by solving a generalized eigenvalue problem, which for a Fourier order of M leads, due to the anisotropy and non-reciprocity to the solving of $4x(2M+1)$ coupled first order equations. After benchmarking this method by using the structure proposed in Ref. 14 we calculated the dispersion relation for the structure shown in Fig. 1 and found that within the frequency range $0.366 < \omega/\omega_p < 0.376$ (ω_p

being the Drude metal bulk plasma frequency) light can propagate only along one direction. The magneto-optically induced one-way frequency range appears (in a first order approximation) via a nonreciprocal splitting of the characteristic surface plasmon-polariton frequency, $\omega_{SP,\pm} = \omega_{SP,0} \pm \Delta\omega_{MO}$ with $\omega_{SP,0} = \omega_p / \sqrt{\varepsilon + 1}$, where the + and - signs correspond to the forward and backward propagating waves with wave vector k and $-k$, respectively, when the magnetic field is applied along the z-axis. We note that the value of the nonreciprocal splitting $\Delta\omega_{MO}$ obtained by using the FMM is in excellent agreement with the result obtained from an analytical model – see Fig. 2(b) described in Section II. Considering the plasma frequency ω_p of typical metals, the permittivity of typical garnets and taking into account that the MO correction is easily several orders of magnitude smaller than the metal plasma frequency [26], the frequency range of the proposed one-way waveguide belongs to the UV part of the optical spectrum. It has been shown that one can decrease effectively the plasma frequency by controlled corrugation of the metal [29]. In this way a one-way waveguide according to this layout could operate in more standard frequency regimes. This possibility remains to be studied, and depends obviously also on the spectral properties of the magneto-optical strength of the considered MO material.

To validate the results obtained by the MO aperiodic Fourier Modal Method [28] and to obtain deeper physical insight into the underlying mechanisms associated with one-way propagation we examine the band structure of the one-way waveguide shown in Fig. 1 by using a simple theoretical model and the plane-wave technique. These methods treat separately both key mechanisms assuring the functionality of the one-way waveguide, namely time-reversal symmetry breaking, which gives rise to the one-way frequency range, and a suppression of disorder-induced backscattering due to the presence of the band gap intrinsic to the photonic crystal. The theoretical model which we use in the first step is based on the analysis of the non-reciprocal surface wave in the Voigt transverse configuration [27]. We assume a simplified waveguide where the photonic crystal in the configuration shown in Fig. 1 is replaced by an uniform MO medium, and we evaluate the dispersion relation for a TM-polarized surface

plasmon-polariton propagating at the interface between the semi-infinite metallic and MO materials. In the second step we neglect an external magnetic field and calculate the band structure associated with the 2D photonic crystal fabricated from the MO material by using a standard plane-wave method. The resulting band structure is obtained when the dispersion relation obtained from the equation for the surface wave propagating at the interface between the metal and the uniform MO material is superimposed on the underlying band structure associated with the 2D MOPhC.

The uniform gyrotropic material in the case of the Voigt transverse configuration is characterized by the permittivity tensor

$$\vec{\vec{\varepsilon}} = \begin{pmatrix} \varepsilon_{xx} & \varepsilon_{xy} & 0 \\ -\varepsilon_{xy} & \varepsilon_{yy} & 0 \\ 0 & 0 & \varepsilon_{zz} \end{pmatrix}, \tag{1}$$

which in the presence of a static magnetic field $\boldsymbol{B}$ in the z direction for a specific MO material such as e.g. bismuth iron garnet is characterized by the permittivity tensor

$$\vec{\vec{\varepsilon}} = \begin{pmatrix} \varepsilon & ig & 0 \\ -ig & \varepsilon & 0 \\ 0 & 0 & \varepsilon \end{pmatrix}, \tag{2}$$

where $\varepsilon = \varepsilon_{xx} = \varepsilon_{yy} = \varepsilon_{zz}$ is the isotropic permittivity of the material and $g = g_z$ is the non-zero component of the gyrotropic vector $g = g1_M$, while $g_x = g_y = 0$. Here 1_M denotes the unit vector along the magnetization direction and g is the gyrotropic constant that enters the expression for the Faraday rotation $\Phi_F = \pi g/n\lambda$, where λ denotes the wavelength and n the refractive index. We note that the signs of the gyrotropic vector components change with time reversal as they are proportional to the magnetization unit vector. We note that the permittivity of the gyrotropic material is chosen to be identical with that of the 2D MOPhC. Since the component of the field

associated the surface wave propagation along the metal/MO interface decays exponentially away from the interface we do not use effective permittivity $\varepsilon_{eff} = f\varepsilon_{MO} + (1-f)\,\varepsilon_0$, where ε_o and ε_{MO} corresponds to the permittivity of the vacuum and of the 2D MOPhC, respectively, and *f* denotes the filling fraction of the MO material.

The surface wave is assumed to propagate along the *x*-axis with the wave number k_x, and the attenuation of the waves in the *y*-direction is defined by the quantities $\kappa_{1,2}$, where the indices 1,2 indicate media in the upper and lower half-spaces, respectively. In the case of TM polarization we consider electric and magnetic field vectors in the form

$$\boldsymbol{E}(\boldsymbol{r},t) = (E_{x1}, E_{y1}, 0)\exp[i(k_x x - \omega t) - \kappa_1 y)]$$

$$\boldsymbol{H}(\boldsymbol{r},t) = (0, 0, H_{z1})\exp[i(k_x x - \omega t) - \kappa_1 y)] \quad \text{for } y>0, \tag{3}$$

while

$$\boldsymbol{E}(\boldsymbol{r},t) = (E_{x2}, E_{y2}, 0)\exp[i(k_x x - \omega t) + \kappa_2 y)]$$

$$\boldsymbol{H}(\boldsymbol{r},t) = (0, 0, H_{z2})\exp[i(k_x x - \omega t) + \kappa_2 y)] \quad \text{for } y < 0. \tag{4}$$

Then Maxwell's equations for the electric-field components reveal that the TM (E_x,E_y,H_z) and TE (H_x,H_y,E_z) modes are uncoupled and only TM polarized modes are affected by the off-diagonal antisymmetric terms $\varepsilon_{xy} = -\varepsilon_{yx}$ giving rise to the nonreciprocity. By using the continuity of the *x*-components of the electric field **E** and the normal components of the displacement vector **D** one obtains the dispersion relation for a gyrotropic surface wave in the form

$$k_x^2 = k_0^2 \frac{K_1 \pm K_2}{(\varepsilon_m^2 - \varepsilon_\nu \varepsilon_{xx})^2 + 4\varepsilon_m^2 \varepsilon_{xy}^2} \quad , \tag{5}$$

where

$$K_1 = (\varepsilon_\nu \varepsilon_{xx} - \varepsilon_m^2)(\varepsilon_\nu - \varepsilon_m)\varepsilon_m \varepsilon_{xx} + 4\varepsilon_m^3 \varepsilon_{xy}^2 \qquad K_2 = 2i\varepsilon_{xy}\varepsilon_m^2 \sqrt{\varepsilon_m \varepsilon_{xx}(2 - (\varepsilon_m^2 + \varepsilon_\nu \varepsilon_{xx}))} \quad . \tag{6}$$

Here we introduced $\varepsilon_v = \varepsilon_{xx} + \varepsilon_{xy}^2 / \varepsilon_{xx}$ and $\varepsilon_m = 1 - \omega_p^2 / \omega^2$ which characterizes a lossless metal described by the Drude free-electron model dielectric function, where ω_p is the plasma frequency.

By using the permittivity tensor (2) with the constant components $\varepsilon = 6.25$ and $g = 0.1$ [26], [30] and the Drude free-electron model dielectric function with, $\omega_p = 1.381 \times 10^{16}$ rad/s, which corresponds to the bulk plasma frequency of silver one obtains from Eq. (5) the dispersion relation for the surface plasmon-polariton. In Fig. 2(b) we present part of the dispersion relation which possesses one-way frequency range within which the SPP can propagate only in one direction. The frequency $\omega_c = \omega_p / \sqrt{\varepsilon + 1}$ associated with the center of the one-way frequency range $0.366 < \omega/\omega_p < 0.376$ corresponds to the frequency of the SPP propagating along the interface in the absence of the external magnetic field.

We note that this one-way frequency range coincides with the one obtained by the Fourier modal method reported by us previously [28]. Thus our theoretical model confirms that the time-reversal symmetry giving rise to magnetic field-induced non-reciprocity and the existence of a one-way frequency range solely relies on the material properties of magnetic medium and implies unidirectional propagation of the surface plasmon-polariton. On the other hand, one has to keep in mind that the periodicity of the MO medium plays a key role in the system. The functionality of the one-way surface waveguide is fully exploited if the radiation continuum is suppressed. Nanostructuring the MO material into a PhC layout that introduces a forbidden frequency gap which contains the one-way frequency range, effectively suppresses any backscattering loss into radiation modes. In order to achieve a sizeable band gap one has to replace a MO medium by a 2D suitable periodic arrangement. Specifically, we consider a 2D MOPhC - see Fig. 1 - consisting of a square array of veins fabricated from bismuth iron garnet characterized *by* $\varepsilon = 6.25$, where the thickness of the veins is $d = 0.23a$, with a the lattice constant, while the square holes are filled with air.

To calculate the band structure for TM polarized waves propagating in the absence of the external magnetic field through an infinite 2D MOPhC we employed a standard plane wave method implemented in the MIT software package [31]. We have found that the band structure along the *Γ-X* direction in the first Brillouin zone reveals a band gap in the frequency range $0.25 < \omega/\omega_p < 0.4$ – see Fig. 2(a) - which accommodates the one-way frequency range $0.366 < \omega/\omega_p < 0.376$ shown in Fig. 2(b). A simplification introduced in our model, namely that the photonic crystal component of the one-way waveguide is evaluated in the absence of the external magnetic field is based on the two following assumptions: i. the finite system consisting of 12 layers that has been considered in the band structure calculations [28] produces a sufficiently accurate approximation of the band structure of the infinite 2D photonic crystal shown in Fig. 2(a); ii. the band structure is not significantly affected due to the presence of the magnetic field. In fact, on the basis of symmetry considerations, it is easy to prove that with the magnetization perpendicular to the plane of the crystal and the crystal motif itself possessing space inversion symmetry, the TM bands of the latter will merely acquire a second order energy correction [32]. A band asymmetry will not appear on these PhC bands themselves. That asymmetry is entirely enclosed in the SPP defect mode within the gap.

The thickness of the veins $d = 0.23a$, which corresponds to the filling fraction of the MO material $f = 0.41$, is chosen to comply with the two-fold role of the MOPhC, namely to provide sufficiently thick veins to give rise to a unidirectional frequency range due to the breaking of time-reversal symmetry, and simultaneously to yield the band gap which the one-way frequency range falls within and which eliminates the radiation modes. To accommodate the SPP one-way frequency range within the band gap expressed in normalized units one has to scale the lattice constant *a*. Specifically, we combine the expression for the midgap frequency $\omega_c = 0.396 \times 2\pi c/a$ determined from the band structure calculation [28] and the frequency of the SPP propagating along the metal/MOPhC interface $\omega_c = \omega_p/\sqrt{\varepsilon+1} = \omega_p/\sqrt{7.25}$ to obtain an appropriate value of the

lattice constant $a = 1.066\lambda p$, where λp denotes the wavelength corresponding to the bulk plasma frequency ω_p.

2. B **GENERALIZED FDTD METHOD.**

In this Section we describe the algorithm based on the standard FDTD [33] method that has been employed to investigate the transport properties of the one-way EM waveguide shown in Fig. 1. Our method implements the tensor form of the magneto-optic permittivity using approaches based on the Z-transform [34] and the ADE algorithm [35]. We assume that the permittivity tensor of the MO material, namely bismuth iron garnet in the presence of the magnetic field $\boldsymbol{B}$ in the z direction, i.e. in the Voigt configuration, is given by Eq. (2). In the case of TM polarization we consider time-dependent electric and magnetic fields $E(\mathbf{r},t) = (E_x, E_y, 0)\exp(-i\omega t)$ and $H(\mathbf{r},t) = (0, 0, H_z)\exp(-i\omega t)$. Then the Maxwell curl equations can be written in the form

$$\nabla \times \vec{E}(r,t) = -\mu_0 \frac{\partial \vec{H}(r,t)}{\partial t} \tag{7}$$

$$\nabla \times \vec{H}(r,t) = \ddot{\sigma}\, \vec{E}(r,t) + \varepsilon_0 \varepsilon(r) \frac{\partial \vec{E}(r,t)}{\partial t}\,, \tag{8}$$

where ε_0 and μ_0 are the permittivity and permeability of vacuum, respectively, and the conductivity tensor $\ddot{\sigma}$ reads as

$$\ddot{\sigma} = \begin{pmatrix} 0 & \omega\varepsilon_0 g & 0 \\ -\omega\varepsilon_0 g & 0 & 0 \\ 0 & 0 & 0 \end{pmatrix}. \tag{9}$$

We discretize Eqs. (7) and (8) with respect to time and space and implement them according to the Z-transform scheme [34]. The metallic part of our one-way waveguide configuration shown in Fig. 1 is described by a Drude free-electron model dielectric function, which accounts for dissipation, and is given by

$$\varepsilon(\omega) = 1 - \frac{\omega_p^2}{\omega(\omega + i\gamma)}, \tag{10}$$

where ω_p is the Drude plasma frequency and $\gamma = 1/\tau_e$ is the inverse electron relaxation time. To implement the frequency-dependent dielectric function given by Eq. (10) within the FDTD method we employed the ADE algorithm [35].

3. NUMERICAL RESULTS.

3. A ONE-WAY PROPAGATION VS. BOUNDARY CONDITIONS IN THE PRESENCE OF A STATIC MAGNETIC FIELD

Recently, we have demonstrated on the basis of numerical simulations [28] that our modified one-way waveguide shown in Fig. 1 supports a one-way frequency range that can be achieved by a substantially smaller magnetic field (~10^1 of mT) than that used in Ref. 14. Here we extend the numerical investigation of this system by studying the influence of specific types of boundary conditions on the one-way functionality. It is worth pointing out that imposing the modified boundary conditions represents qualitatively different factors, in comparison to isolated scatterters placed inside the channel that have been shown to suppress disorder-induced backscattering [14]. Namely, we demonstrate how the surface mode that strongly depends on boundaries (unlike the channel mode considered in Ref. 20) behaves when it bounces off an "infinite-size" wall inside a unidirectional channel. We show that while unidirectionality is independent of the wall termination, the resulting light flow can be controlled when appropriate boundary conditions are imposed.
By referring to the standard case in which perfectly matched layers (PML) are placed on both sides of the interface – see the left panel of Fig. 3(a), we consider two alternative configurations shown in Figs. 3(b), (c). Specifically, we study the waveguide, where the wall fabricated from a perfect conductor (PC) replaces the PML layer at the left boundary – left panel of the Fig. 3(b), and when a

PC wall that is perpendicular to the interface is introduced inside the waveguide configuration in such a way that it cuts the PhC in the middle between two successive MO garnet veins – left panel of Fig. 3(c). We note that the waveguides shown in Fig. 3 represent schematic images of the real computational domains used for the FDTD simulations. As we mentioned in the preceding section the metallic part of the waveguide is described by the Drude free-electron model dielectric function given by Eq. (10) with $\omega_p = 1.381 \times 10^{16}$ rad/s, $\gamma = 6.28 \times 10^{12}$ rad/s, which correspond to the permittivity of silver. The MO material in the PhC is characterized by the permittivity tensor given by Eq. (2) with the constant components $\varepsilon = 6.25$ and $g = 0.1$. The thickness of the vein is $d = 0.23a$, with the lattice constant $a = 1.066\lambda_p$. To demonstrate unidirectional propagation we start with the reference configuration displayed in the left panel in Fig. 3(a). We evaluate the magnetic field distribution of the TE polarized propagating wave excited by a dipole point source placed between the metal and the MOPhC in the waveguide structure – see the right panel of Fig. 3(a). The frequency of the excitation source has been chosen to coincide with the midgap frequency $\omega_c = \omega_p/\sqrt{7.25}$, where ω_p is the Drude bulk plasma frequency. The magnetic field associated with this surface mode possesses a localized nature, i.e. it is confined along the metal/MOPhC interface, and reveals negligible attenuation along the interface within the range of 12 periods considered in the computational domain, and confirms the absence of backreflection. We note that since the absorption of the bismuth iron garnet in the frequency range considered in comparison with the size of the off-diagonal component of the permittivity tensor is negligible [26],[30], we assume in our model that the MO material is lossless. However, our method in principle allows considering a lossy MO material with a realistic damping parameter. By placing the detectors at the interface in the direction where propagation is not allowed we found that the unidirectional wavelength range occurs within 360 nm $< \lambda <$ 380 nm. The one-way frequency range is somewhat wider than that obtained from the band structure calculation $0.366 < \omega/\omega_p < 0.376$, which corresponds to the wavelength range 363 nm $< \lambda <$ 373 nm. Finally, we investigate how the one-way property is affected when boundary conditions are modified by presenting the magnetic field distribution along the metal/MOPhC

interface – see the right panel of Fig. 3(b) - associated with the configuration depicted in left panel of Fig. 3(b). One can see that placing the perfect conductor wall in such a way that it coincides with the boundary of the unit cell of the photonic crystal leads to the propagation in the perpendicular directions along the $y+$ and $x+$-axes which would result in a complete circulation of the light along the boundaries (provided the PML layer on the right boundary is replaced by a PC wall). We also note that the magnetic field associated with the surface mode propagating along the y^+ and x^+ axes reveals a modified confinement in comparison with that corresponding to the metal/MOPhC interface. This surface mode is obviously not a plasmon-polariton since it is not guided by the PEC interface but by the high index vein and the bandgap structure lying next to it. The fact that all the forward guided SPP light bouncing of the PEC wall gets channeled into this numerically induced PhC surface mode proves the absence of a backward channel in the SPP waveguide. In contrast to the previous case, the propagation of light along the metal/MOPhC interface is completely stopped when the PC wall is introduced inside the waveguide in such a way that it cuts the PhC in the middle between the veins. By cutting the PhC in this way the previously accessible PhC surface state is no longer accessible since there is no continuous high index layer between the crystal and the PEC wall. In the right panel of Fig. 3(c) we present the distribution of the magnetic field with the midgap frequency ω_c which, in contrast to configuration depicted in Fig. 3(b), does not show circulation along the metal wall and rather reveals strong scattering into the evanescent modes of the photonic crystal while backscattering is suppressed.

3. B TRANSPORT AND SPECTRAL PROPERTIES IN THE PRESENCE OF A TIME-DEPENDENT MAGNETIC FIELD.

To explore alternative possibilities of controlling the propagation of the SPP within a one-way waveguide we also examined its dynamical properties in the presence of a time-dependent magnetic field. Namely we consider a harmonically oscillating field in the form $B(t) = \Delta B \sin\omega_e t$. Here ω_e is

the modulation frequency of the external magnetic field, the strength of the modulation ΔB is within the range $0 < \Delta B < \Delta B_{max}$,where ΔB_{max} is the amplitude of the modulation which corresponds to the magnetization associated with the off-diagonal term $g = 1$ belonging to the permittivity tensor given by Eq. (2). We also inspect the case when the static magnetic field $B(t) = \Delta B$, $t<t_{0,}$ is switched off at some time t_0, i.e. possessing the Heaviside step function behavior. The modulation frequency of the external magnetic field ω_e in the former case is chosen to be an order of magnitude smaller than that of the frequency of the oscillating dipole that has been chosen to coincide with the midgap frequency $\omega_c = 0.396 \times 2\pi c/a$ in normalized units. To demonstrate the behavior of the propagating light in the waveguide we present in Fig. 4 two snapshots of the distribution of the energy density after 10 periods of modulation of a sinusoidal time-dependent external magnetic field. The distributions shown in Figs. 4(a) and (b) correspond to instantaneous values of the modulation $B(t_a) = 0.5\Delta B_{max}$ and $B(t_b) = -0.5\Delta B_{max}$, respectively, that are indicated by the full circles on the curve displayed in Fig. 4(c). The magnetic fields shown in Figs. 4(a),(b) can be divided into three regions which represent separated domains of the field distributions associated with the mode which arise due to the modulation of the external magnetic field. Specifically, in Fig. 4(b), which corresponds to an instantaneous modulation $B(t_b) = -0.5\Delta B_{max}$, one can identify the fraction of the energy density which starts to propagate (due to the opposite sign of the external magnetic field) in the reverse direction i.e. to the left, while in the central part, which is placed on the right side from the position of the oscillating dipole, is the energy density which represents the non-propagating fraction. We note that this feature has not been observed in the case of a step-like modulation(not shown here). The field distribution on the right side of the panel in Fig. 4(b) corresponds to the part of the wave which curiously enough continues to propagate in the forward direction and, therefore, can be assigned to an induced mode which we inspect in more detail below. In Fig. 4(a) we show the snapshot of the energy density that corresponds to the instantaneous modulation $B(t_a) = 0.5\Delta B_{max}$ that is indicated by the full circle in Fig. 4(c). One can see that the distribution of the energy density reveals the same behavior as that associated with the opposite sign of the modulation shown in Fig.

4(b) and the pattern is symmetric with respect to the line parallel with the y-axis that crosses the interface at the position of the dipole. To inspect the nature of the modes observed in more detail we carried out a series of numerical experiments in which we studied the Fourier spectrum of the field within the structure. Namely, by evaluating the Fourier transform of the energy density we explored the dependence of the energy density on the amplitude of the modulation of the external magnetic field and on the frequency of the modulation. The results obtained for the case of the sinusoidal modulation are summarized in Fig. 5. The left panel in Fig. 5 shows part of the band structure which contains the intrinsic PhC band gap (light shaded region) which accommodates a unidirectional frequency range (dark shaded range). On the right panel we display Fourier transforms of the EM energy density of the modes which characterize spectra as they depend on the amplitude of the modulation of the external magnetic field ΔB in units related to the off-diagonal term g belonging to the permittivity tensor given by Eq. (2). The spectrum on the left side of the right panel, which corresponds to a small modulation ~1%, reveals a single peak and thus indicates that unidirectional propagation is not affected. When the strength of the modulation ΔB is increased in the range $0.01\Delta B_{max} < \Delta B < \Delta B_{max}$ a number of replicas of the modes appear in the spectrum. We note that when the number of the induced modes exceeds two side lobes, the system enters a nonlinear regime characterized by an increasing number of induced modes. Simultaneously, the induced modes mutually interact and display a dependence of their amplitudes on the strength of the modulation ΔB. The number of modes within the frequency range considered can be controlled by varying the frequency of the modulation. We have demonstrated numerically for the frequencies lower or higher than the reference one $\omega_e = 0.1\omega_c$ that the number of the modes is inversely proportional to the frequency of the modulation(not shown here). We note that in the case of a step-like modulation of the external magnetic field the spectrum in comparison with sinusoidal case is significantly different, namely it does not contain the localized states within the stop band, and this feature is consistent with the absence of the central part of the distributions of the energy density shown in Figs. 4(a) and (b).

The Fourier components of the energy density shown in Fig. 5 can be used in the interpretation of the specific features such as, for example, the induced modes that can be distinguished in the energy density patterns shown in Fig. 4. For the specific case considered that is defined by the ratio between the modulation frequency of the external magnetic field and that of the oscillating dipole given by $\omega_e = 0.1\omega_c$ there exists only a single mode with the central frequency which falls inside the unidirectional frequency range. All other induced modes are either exponentially decaying waves with frequencies within the intrinsic PhC gap that correspond to localized modes, or are extended-like modes with frequencies within allowed bands. We claim that the latter modes can be identified as induced modes shown in Figs. 4(a),(b). It is worth noting that the equidistant frequency levels in the spectra observed in Fig. 5 resemble a series of virtual states in quantum systems whose energy is equally spaced known as Wannier-Stark resonances [36] that occur in crystals in the presence of a uniform external electric field for an electron moving in the periodic potential. The resonances presented in Fig. 5 can be considered as a photonic analogue of its electronic counterpart which, in contrast to previously reported optical Wannier-Stark ladder systems[37]-[39], are implied to be due to the time-dependent modulation of the external magnetic field.

4. DISCUSSION AND CONCLUSION.

We have proposed an improved concept of a one-way device which can be used for the design of compact integrated analogues of one-way electronic devices such as diodes and transistors. The configuration which we consider allows using a small external magnetic field. We studied the underlying dispersion relations and transport properties of the SPP in the presence of a static and/or time-dependent external magnetic field. In particular in the presence of a time-dependent magnetic field we found interesting features of the field pattern associated with the SPP that may offer new mechanisms for dynamical control of its flow. In order to accomplish the design that would be fully competitive with standard electronic counterparts one

needs to scale frequencies to the telecom range. As we mentioned in Sec. I, the operating frequency of the one-way waveguide considered depends on the material properties of the metal, and typically offers a one-way frequency range in the visible or ultraviolet parts of the spectrum. We have shown recently [40] that this restriction can be avoided when acoustic plasmons [41-43] are employed instead of regular surface plasmons, and this concept enables creating a one-way waveguide structure in the terahertz frequency range. We numerally examined the unidirectional transport properties of the modified one-way waveguide in the terahertz regime based on the propagation of the acoustic plasmons at the metal/PhC interface. Likewise we proved that it offers a viable alternative to propagation of the SPP at terahertz frequencies based on the concept of spoof plasmons [29] that has been the subject of intensive investigation recently. In conclusion, we have studied both theoretically and numerically a nonreciprocal waveguide that relies on time-reversal symmetry breaking implied by the photonic crystal fabricated from a MO material subjected an external magnetic field. We have shown that such a configuration allows achieving sizable one-way bandwidth by using significantly smaller values of the external magnetic field than the previously reported system [14]. We have implemented a simple theoretical model that validates the results obtained by the aperiodic Fourier Modal Method MO, a-FMM, and provides deeper physical insight into the phenomena associated with non-reciprocity introduced by the MO properties of the magneto-optic photonic crystal. By using a generalized version of the FDTD method we studied the dynamical properties associated with the propagation of EM waves through media with tensor magneto-optic permittivity. Namely, in the presence of a static external magnetic field we studied the influence of specific types of boundary conditions on one-way functionality. We found that the behaviour of a one-way waveguide is strongly affected by the presence of a time-dependent external magnetic field, which gives rise to new and interesting features associated with the redistribution of the EM field, and interpret them in terms of the Fourier transform of the EM energy density.

Acknowledgement.

V.K. acknowledges support of the Grant No. OC09060 of Czech Ministry of Education within COST Action MP0702. V.K. and S.E. acknowledge support of the National Science Foundation of the Czech Republic by the Grant No. P205/10/0046. We greatly acknowledge thorough reading of our manuscript by Prof. A. A. Maradudin prior to its resubmission.

REFERENCES.

1. S. John, Phys. Rev. Lett. **58**, 2486 (1987).

2. E. Yablonovitch, Phys. Rev. Lett. **58**, 2059 (1987).

3. F. D. M. Haldane and S. Raghu, *arXiv:cond-mat/0503588v1*; F. D. M. Haldane and S. Raghu, Phys. Rev. Lett. **100**, 013904 (2008).

4. K. von Klitzing, K. Dorda, and M. Pepper, Phys. Rev. Lett. 45, 494 (1980).

5. Z. Wang, Y. D. Chong, J. D. Joannopoulos, and M. Soljacic, Phys. Rev. Lett. **100**, 013905 (2008).

6 Z. Wang, Y. Chong, J. D. Joannopoulos, and M. Soljacić, Nature **461**, 772 (2009).

7 T. Ochiai and M. Onoda, Phys. Rev. B **80**, 155103 (2009).

8 E. Yablonovitch, Nature **461**, 744 (2009).

9. I. Vitebsky, J. Edelkind, E. N. Bogachek, A. G. Scherbakov, and U. Landman, Phys. Rev. B **55**, 12566 (1997).

10. A.Figotin and I.Vitebsky, Phys. Rev. E **63**, 066609 (2001).

11. A.Figotin and I.Vitebskiy, Phys. Rev. B **67**, 165210 (2003).

12. Z. Yu, G. Z. Wang, and S. Fan, Appl. Phys. Lett. **90**, 121133 (2007).

13. A. B. Khanikaev and M. J. Steel, Opt. Express. **17**, 5265 (2009).

14. Z. Yu, G. Veronis, Z. Wang, and S. Fan, Phys. Rev. Lett. **100**, 023902 (2008).

15. H. Takeda and S. John, Phys. Rev. A **78**, 023804 (2008).

16. Z. Wang and S. Fan, Appl. Phys. Lett. B, Laser Opt. **81**, 369 (2005).

17. Z. Wang and S. Fan, Opt. Lett. **30**, 1989 (2005).

18. M. Vanwolleghem, X. Checoury, W. Smigaj, B. Gralak, L. Magdenko, K. Postava, B. Dagens, P. Beauvillain, and J. M. Lourtioz, Phys. Rev. B **80**, 121102 (2009).

19. A. B. Khanikaev and M. J. Steel, PNMA **8**, 125, (2010).

20 W.J. Chen, Z. H. Hang, J.W. Dong, X. Xiao, H.Z. Wang, and C.T. Chan, Phys. Rev. Lett. **107**, 023901 (2011).

21. J. Hwang, M. H. Song, B. Park, S. Nishimura, T. Toyooka, J. W. Wu, Y. Takanishi, K. Ishikawa, and H. Takezoe, Nature Materials **4**, 383 (2005).

22 M. H.Song, B. Park, S. Nishimura, T. Toyooka, I. J. Chung,Y. Takanishi, K. Ishikawa, and H. Takezoe, Advanced Functional Materials **16**, 1793 (2006).

23 L. Feng, M. Ayache, J. Huang, Y.L. Xu, M.H. Lu, Y.F. Chen, Y. Fainman, and A. Scherer, Science **333**, 729(2011).

24 A. E. Serebryannikov and E. Ozbay, Opt. Express **17**, 13335 (2009).

25. S. Fan, R. Baets, A. Petrov, Z. Yu, J. D. Joannopoulos, W. Freude, A. Melloni, M, Popović, M. Vanwolleghem, D. Jalas, M. Eich, M. Krause, H. Renner, E. Brinkmeyer, C. R. Doerr, Science, **335**, 38(2012)

26 B. Vertruyen, R. Cloots, J. S. Abell, T. J. Jackson, R. C. da Silva, E. Popova, and N. Keller, Phys. Rev. B **78**, 094429, (2008).

27. A. Boardman, N. King, Y. Rapoport, and L.Velasco New J. Phys. **7,** 191(2006).

28 S. Eyderman, V. Kuzmiak, and M. Vanwolleghem, in *Proc. SPIE Vol. 7713 Photonics Europe Photonic Crystal Materials and Devices IX*, 77130P-1.

29. B. Pendry, J. B. Martin-Moreno, and F.J. Garcia-Vidal, Science **305**, 847-848(2005).

30. T. Tepper and C. Ross, J. Cryst. Growth., **255**. 324 (2003).

31. A. F. Oskooi, D. Roundy, M. Ibanescu, P. Bermel, J. D. Joannopoulos, and S. G. Johnson, Computer Physics Communications **181**, 687 (2010).

32. M. Vanwolleghem, P. Gogol, P. Beauvillain, and J. Lourtioz, *in Conference on Lasers and Electro-Optics/Quantum Electronics and Laser Science Conference and Photonic Applications Systems Technologies*, Technical Digest (CD) (Optical Society of America, 2006), paper QTuC2.

33. K. S. Yee, IEEE. Trans. Antennas Propagat. **14**, 14 (1966).

34. S. J. Huang and F. Li, Comp.Phys. Comm., 166. 45 (2005).

35. Y. Zhao, Ch. Argyropuolos, and Y. Hao, arXiv:0803.2063v1.

36. G. H. Wannier, Phys. Rev. **117,** 432 (1960).

37. G. Monsivais, M. delCastillo-Mussot, and F. Claro,, Phys. Rev. Lett. **64**, 1433 (1990).

38. C. M. deSterke, J. N. Bright, P. A. Krug, and T. E. Hammon,, Phys. Rev. E **57**, 2365 (1998).

39. S. R. Wilkinson, C. F. Bharucha, K. W. Madison, Q. Niu, and M. G. Raizen, Phys. Rev. Lett. **76**, 4512 (1996).

40. S. Eyderman, V. Kuzmiak, and M. Vanwolleghem, ICTON: 2011 13TH INTERNATIONAL CONFERENCE ON TRANSPARENT OPTICAL NETWORKS, VOL. 1, 411, 2011.

41. V.M Silkin, J.M.Pitarke, E.V.Chulkov, and P. M. Echenique, Phys. Rev. B **72**, 115435 (2005).

42. J.M.Pitarke, M.V. Silkin, E.V.Chulkov, and P. M. Echenique, J. Opt. A: Pure Appl. Opt **7**, S73-S84 (2005).

43. B. Diagonescu, K. Pohl, L.Vattuone,L. Savio, P. Hofman,V. M. Silkin, J. Pitarke, E. V. Chulkov, P. M. Echenique, D. Farias, and M. Rocca ,Nature **448**, 57(2007).

Figure Captions

Figure 1 : (color online) One-way waveguide formed by a metal/MOPhC interface. The thickness of the vein $d = 0.23a$, where a is the lattice constant.

Figure 2 : (color online) (a) The photonic band structure of the infinite 2D photonic crystal consisting of a square array of veins fabricated from bismuth iron garnet while the square holes are filled with air; (b) Nonreciprocal surface wave dispersion relation for a surface plasmon polariton propagating between the metal and bismuth iron garnet, which possesses a one-way frequency range $0.366 < \omega/\omega_p < 0.376$.

Figure 3 : (color online) (a) One-way waveguide configuration formed by a metal/MOPhC interface with PML absorbers(left panel); modified waveguides(left panels) (b) with the wall fabricated from a perfect conductor(PC) at the left and upper boundaries, (c) with the PC wall embedded perpendicular to the one-way interface. On the right panels the magnetic field distribution of a propagating wave at the frequency $\omega_c = \omega_p/\sqrt{7.25}$ inside the gap in the corresponding waveguide structures are shown.

Figure 4 : (color online) Snapshots in (a) and (b) of the magnetic field which shows the redistribution of the EM energy density due to the presence of the time-dependent external magnetic field that correspond to the instantaneous values of the modulation $B(t_a) = 0.5\Delta B_{max}$ and $B(t_b) = -0.5\Delta B_{max}$ that are indicated by the full circles on the curve displayed in the panel at the bottom of (a).

Figure 5 : (color online) The photonic band structure of the MOPhC with a one-way frequency range(left panel) vs. Fourier transforms of the EM energy density of the modes as functions of the strength of the modulation of the time-dependent external magnetic field ΔB.

FIGURE 1

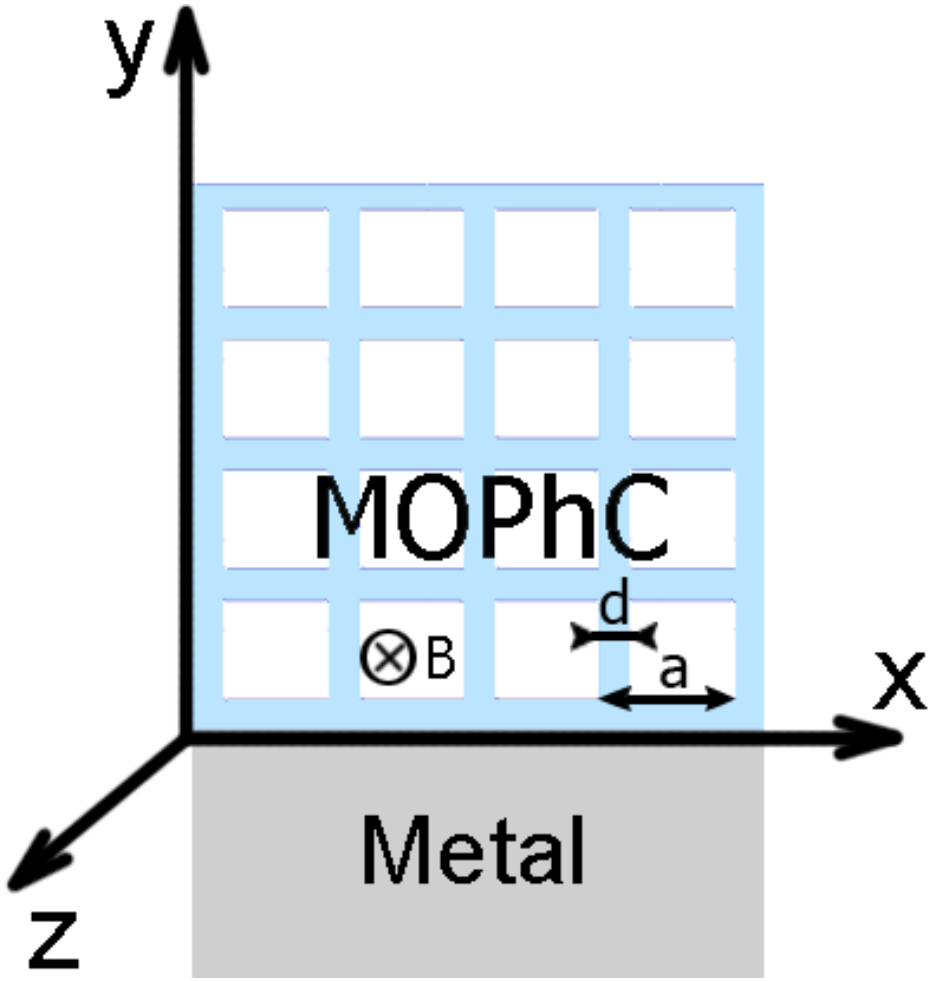

FIGURE 2.

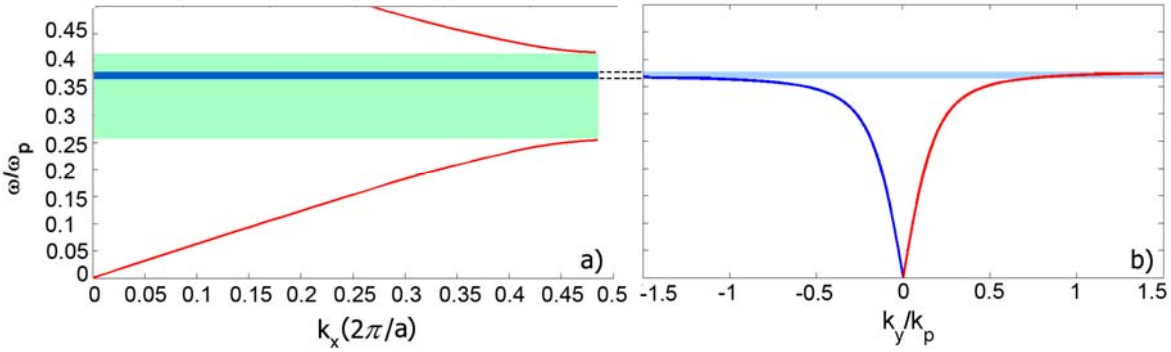
0.45
0.4
0.35
0.3
0.25
0.2
0.15
0.1
0.05
0
ω/ω_p
0 0.05 0.1 0.15 0.2 0.25 0.3 0.35 0.4 0.45 0.5
k_x(2π/a)
a)
-1.5 -1 -0.5 0 0.5 1 1.5
k_y/k_p
b)

FIGURE 3.

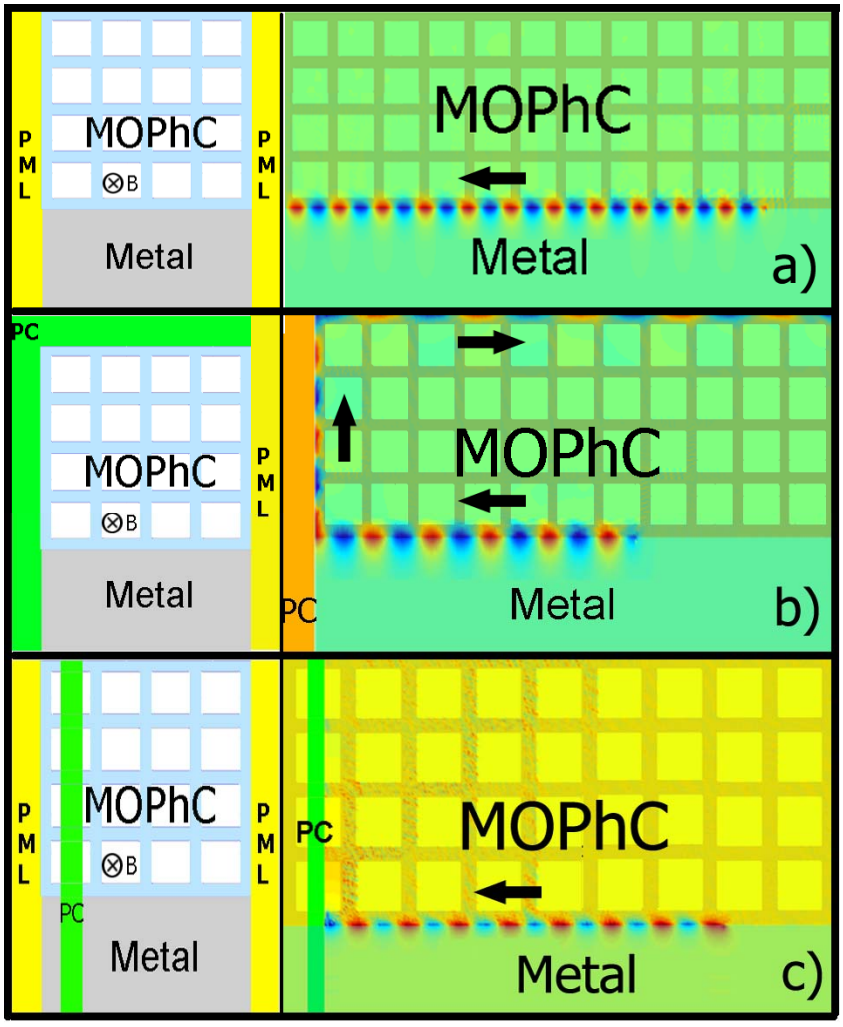
PML
MOPhC
⊗B
Metal
PML
MOPhC
Metal
a)
PC
PML
MOPhC
⊗B
Metal
PML
MOPhC
PC
Metal
b)
PML
MOPhC
⊗B
PC
Metal
PML
PC
MOPhC
Metal
c)

FIGURE 4

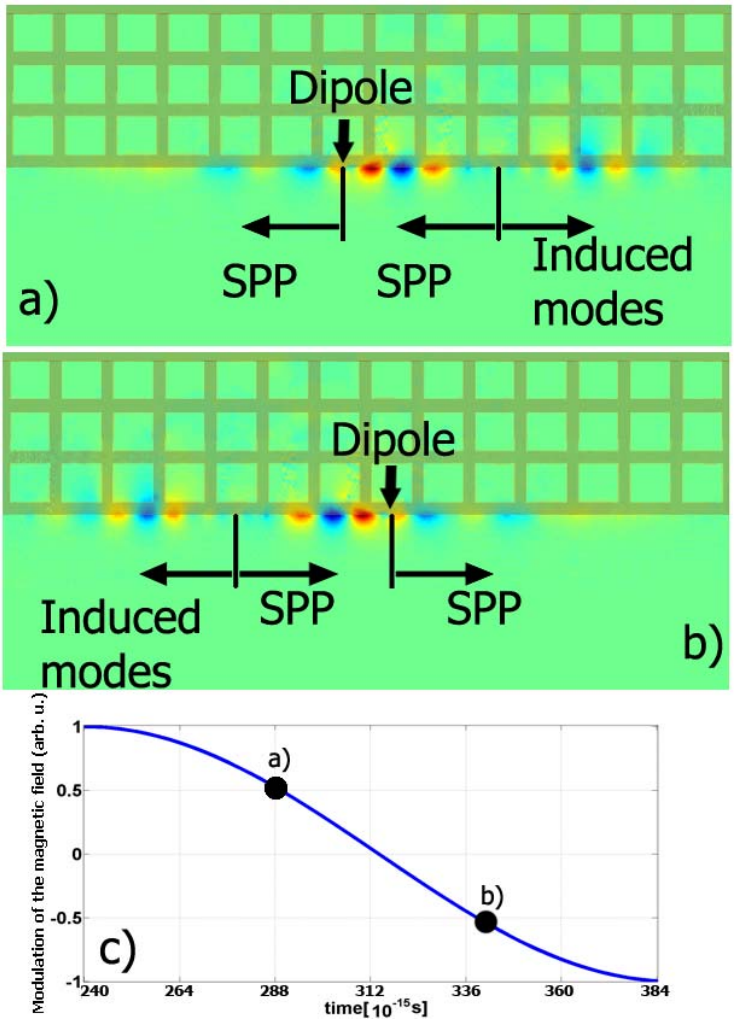
Dipole
SPP
SPP
Induced modes
a)
Dipole
Induced modes
SPP
SPP
b)
Modulation of the magnetic field (arb. u.)
1
0.5
0
-0.5
-1
a)
b)
c)
240
264
288
312
336
360
384
time[10^-15s]

FIGURE 5.

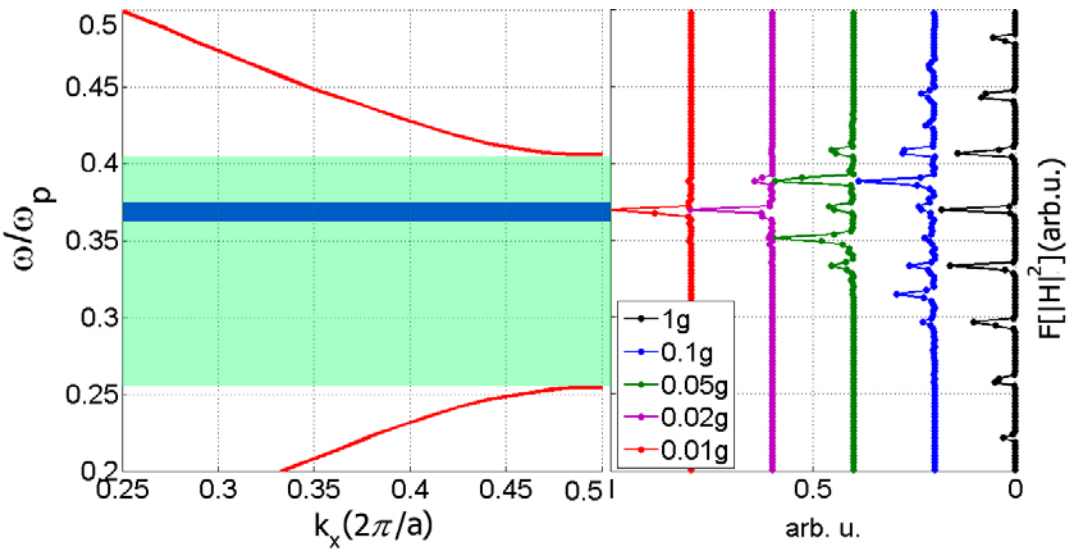
0.5
0.45
0.4
0.35
0.3
0.25
0.2
ω/ω_p
0.25
0.3
0.35
0.4
0.45
0.5
k_x(2π/a)
1g
0.1g
0.05g
0.02g
0.01g
0.5
0
arb. u.
F[|H|^2](arb.u.)